図2　先進医療における膵島移植の免疫抑制療法

たはrapamycinを用い，ステロイドをまったく使用しないレジメで100例 対 100例のヒストリカル試験を報告している[8]．6年の観察で膵，腎とも生着率はステロイド使用群との差はなく，サイトメガロウイルス(CMV)感染症の発症率が有意に低かった．また移植12カ月後の急性拒絶反応発症率も有意に低かった(4.0% vs 14.0%)が，これはステロイドを使用しない群での導入にrATGやalemtuzumabを使用しているためと推察している．

膵臓移植における導入療法はrATGやalemtuzumabの有用性に関する報告が多い．なおalemtuzumabは日本で販売されておらず，海外でも2012年末現在，市販されていない．Bazerbachiらは，同時期に施行した膵腎同時移植において49例のBXM使用群と79例のrATG使用群を比較検討している[9]．膵，腎とも生着率，合併症の頻度に差はなかったが，急性拒絶反応発症率は移植3カ月後，12カ月後ともrATG群で有意に低く(6% vs 21%；P=0.01，14% vs 27%；P=0.049)ステロイド抵抗性拒絶反応発症率はさらに低い(3% vs 14%；P=0.01)と報告している．

膵臓移植において，本邦ではまだ保険適応とされていないが，rATGを導入に用いることが有用である．ステロイド中止または回避には必須と思われる．MMFがその副作用などにより使用困難な場合は，mTOR阻害薬(本邦ではeverolimus)の使用を考慮してもよいと思われる．

膵島移植における免疫抑制療法の変遷

膵島移植における免疫抑制療法は，2000年ころまで腎移植と同様，CyA，アザチオプリン，ステロイドなどであり[10]，この時代の膵島移植1年後のインスリン離脱率は10%弱と，良好とはいえなかった．エドモントンプロトコールではステロイドを使用せず，Tacとrapamycin，導入にdaclizumabを用いるものであり[2]，1年後のインスリン離脱率は飛躍的に改善したが，3年後では20%強と長期成績では満足のいくものではなかった[3]．Eichらのポジトロン CTを用いた研究によると，門脈内に移植した膵島はその約半数が移植直後に消失するとされており[11]，これは主にinstant blood-mediated inflammatory reaction(IBMIR)とよばれる移植直後に引き起こされる血栓性および炎症性反応によるものとされる．Bellinらミネソタ大学のグループは，導入にrATGに加え，TNF-α阻害剤であるetanerceptを用いるプロトコールにて1, 2人のドナーからの移植6例のうち4例が長期にわたってインスリン離脱を得ていると報告している[12]．

先進医療における膵島移植の免疫抑制療法

わが国で再開された膵島移植は基本的に先進医療にて行われており，よって免疫抑制療法もそのプロトコールが決められている．前述のミネソタ

大学のプロトコールに準じているが，evelorimus はMMFに変更されている(図2)．

CyAは6 mg/kgで開始し目標トラフは150～200 ng/mL，Tacの場合は2 mg/dayで開始し目標トラフを3～6 ng/mLとする．MMFは500 mg/dayで開始し，副作用をみながら維持を500～1,500 mgとする．またetanerceptは移植1時間前，移植後3，7，10日目に25 mgを皮下注射する．rATGは移植12時間前から初回投与量として0.5 mg/kgを12時間かけて投与し，さらに移植開始時から12時間かけて1.83 mg/kgを投与する．その後はそれぞれ12時間の休薬ののちに2回投与する．つまり0.5 mg/kgを1回，1.83 mg/kgを3回投与することとなり，総投与量は6 mg/kgとなる．2回目の移植以降はrATGが投与不可能であるため，BXMに置き換える．

わが国では臨床膵島移植再開の体制が整ったものの，2012年末現在，同種移植例はまだない．この新しい免疫抑制プロトコールでの移植成績が期待される．

文　献

1) 日本膵・膵島移植研究会膵臓移植班．本邦膵移植症例報告(2012)．移植　47：437-442，2012
2) Shapiro AM, Lakey JR, Ryan EA, Korbutt GS, Toth E, Warnock GL, Kneteman NM, Rajotte RV. Islet transplantation in seven patients with type 1 diabetes mellitus using a glucocorticoid-free immunosuppressive regimen. N Engl J Med　27：230-238, 2000
3) Ryan EA, Paty BW, Senior PA, Bigam D, Alfadhli E, Kneteman NM, Lakey JR, Shapiro AM. Five-year follow-up after clinical islet transplantation. Diabetes　54：2060-2069, 2005
4) Saito T, Anazawa T, Gotoh M, Uemoto S, Kenmochi T, Kuroda Y, Satomi S, Itoh T, Yasunami Y, Kitamoto T, Mohri S, Teraoka S. Actions of the Japanese Pancreas and Islet Transplantation Association regarding transplanted human islets isolated using Liberase HI. Transplant Proc　42：4213-4216, 2010
5) Ciancio G, Sageshima J, Chen L, Gaynor JJ, Hanson L, Tueros L, Montenora-Velarde E, Gomez C, Kupin W, Guerra G, Mattiazzi A, Fornoni A, Pugliese A, Roth D, Wolf M, Burke GW 3rd. Advantage of rapamycin over mycophenolate mofetil when used with tacrolimus for simultaneous pancreas kidney transplants：randomized, single-center trial at 10 years. Am J Transplant　12：3363-3376, 2012
6) Gruessner AC. 2011 update on pancreas transplantation：comprehensive trend analysis of 25,000 cases followed up over the course of twenty-four years at the International Pancreas Transplant Registry (IPTR). Rev Diabet Stud　8：6-16, 2011
7) Malheiro J, Martins L, Fonseca I, Gomes AM, Santos J, Dias L, Dores J, Oliveira F, Seca R, Almeida R, Henriques A, Cabrita A, Teixeira M. Steroid withdrawal in simultaneous pancreas-kidney transplantation：a 7-year report. Transplant Proc　41：909-912, 2009
8) Axelrod D, Leventhal JR, Gallon LG, Parker MA, Kaufman DB. Reduction of CMV disease with steroid-free immunosuppresssion in simultaneous pancreas-kidney transplant recipients. Am J Transplant　5：1423-1429, 2005
9) Bazerbachi F, Selzner M, Boehnert MU, Marquez MA, Norgate A, McGilvray ID, Schiff J, Cattral MS. Thymoglobulin versus basiliximab induction therapy for simultaneous kidney-pancreas transplantation：impact on rejection, graft function, and long-term outcome. Transplantation　92：1039-1043, 2011
10) Brunicardi FC, Atiya A, Stock P, Kenmochi T, Une S, Benhamou PY, Watt PC, Miyamato M, Wantanabe Y, Nomura Y, et al. Clinical islet transplantation experience of the University of California Islet Transplant Consortium. Surgery　118：967-971, 1995
11) Eich T, Eriksson O, Lundgren T. Visualization of early engraftment in clinical islet transplantation by positron-emission tomography. N Engl J Med　356：2754-2755, 2007
12) Bellin MD, Kandaswamy R, Parkey J, Zhang HJ, Liu B, Ihm SH, Ansite JD, Witson J, Bansal-Pakala P, Balamurugan AN, Papas KK, Sutherland DE, Moran A, Hering BJ. Prolonged insulin independence after islet allotransplants in recipients with type 1 diabetes. Am J Transplant　8：2463-2470, 2008

本稿は，2012年11月16, 17日に福島市・コラッセふくしまで行われた，第39回日本臓器保存生物医学会学術集会シンポジウムIII“免疫抑制療法 up to date”における発表をもとに書き下ろしたものである．

別刷請求先：丸山通広
〒260-8712　千葉県千葉市中央区仁戸名673番地
国立病院機構千葉東病院外科
Tel：043-261-5171．Fax：043-268-2613
E-mail：maruyama@cehpnet.com

Hindawi Publishing Corporation
Disease Markers
Volume 35 (2013), Issue 5, Pages 573–579
http://dx.doi.org/10.1155/2013/392578

Research Article

CD90- (Thy-1-) High Selection Enhances Reprogramming Capacity of Murine Adipose-Derived Mesenchymal Stem Cells

Koichi Kawamoto,[1] Masamitsu Konno,[2] Hiroaki Nagano,[2] Shimpei Nishikawa,[2] Yoshito Tomimaru,[2] Hirofumi Akita,[2] Naoki Hama,[2] Hiroshi Wada,[2] Shogo Kobayashi,[2] Hidetoshi Eguchi,[2] Masahiro Tanemura,[3] Toshinori Ito,[4] Yuichiro Doki,[1] Masaki Mori,[1] and Hideshi Ishii[2]

[1] *Department of Surgery, Graduate School of Medicine, Osaka University, 2-2 Yamadaoka, Suita, Osaka 565-0871, Japan*
[2] *Department of Frontier Science for Cancer and Chemotherapy, Graduate School of Medicine, Osaka University, 2-2 Yamadaoka, Suita, Osaka 565-0871, Japan*
[3] *Department of Surgery and Institute for Clinical Research, National Hospital Organization Kure Medical Center and Chugoku Cancer Center, Hiroshima 737-0023, Japan*
[4] *Department of Complementary and Alternative Medicine, Graduate School of Medicine, Osaka University, 2-2 Yamadaoka, Suita, Osaka 565-0871, Japan*

Correspondence should be addressed to Hiroaki Nagano; hnagano@gesurg.med.osaka-u.ac.jp and Hideshi Ishii; hishii@gesurg.med.osaka-u.ac.jp

Received 18 June 2013; Revised 7 September 2013; Accepted 12 September 2013

Academic Editor: Chao Hung Hung

Background. Mesenchymal stem cells (MSCs), including adipose tissue-derived mesenchymal stem cells (ADSC), are multipotent and can differentiate into various cell types possessing unique immunomodulatory features. Several clinical trials have demonstrated the safety and possible efficacy of MSCs in organ transplantation. Thus, stem cell therapy is promising for tolerance induction. In this study, we assessed the reprogramming capacity of murine ADSCs and found that CD90 (Thy-1), originally discovered as a thymocyte antigen, could be a useful marker for cell therapy. *Method.* Murine ADSCs were isolated from B6 mice, sorted using a FACSAria cell sorter by selection of $CD90^{Hi}$ or $CD90^{Lo}$, and then transduced with four standard factors (4F; Oct4, Sox2, Klf4, and c-Myc). *Results.* Unsorted, $CD90^{Hi}$-sorted, and $CD90^{Lo}$-sorted murine ADSCs were reprogrammed using standard 4F transduction. $CD90^{Hi}$ ADSCs showed increased numbers of alkaline phosphatase-positive colonies compared with $CD90^{Lo}$ ADSCs. The relative reprogramming efficiencies of unsorted, $CD90^{Hi}$-sorted, and $CD90^{Lo}$-sorted ADSCs were 100%, 116.5%, and 74.7%, respectively. $CD90^{Hi}$ cells were more responsive to reprogramming. *Conclusion.* $CD90^{Hi}$ ADSCs had greater reprogramming capacity than $CD90^{Lo}$ ADSCs, suggesting that ADSCs have heterogeneous subpopulations. Thus, $CD90^{Hi}$ selection presents an effective strategy to isolate a highly suppressive subpopulation for stem cell-based tolerance induction therapy.

1. Introduction

Induced pluripotent stem (iPS) cells can be directly generated from fibroblast cultures by expression of four factors (4F), including octamer-binding transcription factor 4, sex-determining region Y-box 2, Kruppel-like factor 4, and myelocytomatosis viral oncogene homolog [1]. Although these factors present attractive sources for stem cell therapy, the mechanisms by which they are generated are not fully understood. The inefficiency of iPS cell generation has prompted the development of two contending models, namely, the stochastic and elite models. A recent multilineage-differentiating stress-enduring cell study suggested the greater utility of the elite model over the stochastic model [2]. In either model, stem cells or progenitor cells isolated for experimental or therapeutic research are usually heterogeneous populations; therefore, a more favorable subfraction for use in stem cell therapy may

exist. Indeed, several reports have suggested that the differentiation stage of the starting cell line has a critical influence on the efficiency of reprogramming into iPS cells in hematopoiesis [3]. Immature cell populations, such as lin$^-$c-Kit$^+$Sca1$^+$CD48$^-$CD150$^+$CD34$^-$ (lack of lineage/Hardy-Zuckerman 4 feline sarcoma viral oncogene homolog/spinocerebellar ataxia/cluster of differentiation 48$^-$/150$^+$/34$^-$) hematopoietic stem cells, in general give rise to iPS cells at higher efficiencies than terminally differentiated cell types. Furthermore, a recent study demonstrated that CD90^{Hi} adipose tissue-derived mesenchymal stem cells (ADSCs) are more capable of forming bone both *in vitro* and *in vivo* than in CD105^{Lo} cells [4]. CD90 (Thy-1) is a 25–37-kDa glycosylphosphatidylinositol-anchored glycoprotein expressed mainly in leukocytes that have been used as murine pan T-cell markers, like CD2, CD5, and CD28.

Multipotent mesenchymal stem cells (MSCs), which represent a nonhematopoietic cell population, can differentiate into mesenchymal tissues (i.e., bone, cartilage, or fat) [5, 6]; they were first isolated from bone marrow and later from nonmarrow tissues, including umbilical cord blood and adipose tissue [5, 6]. Immunologically, MCSs are known to be less immunogenic because of, at least in part, the lack of surface-expressed human leukocyte antigens [5]. Moreover, they have been shown to possess anti-inflammatory and immunosuppressive effects both in murine and human models of diabetes [7, 8]. Thus, the immunoregulatory properties of MSCs are appealing, because they inhibit T-cell proliferation and differentiation of monocytes to dendritic cells, modulate B-cell functions, and suppress natural killer cell cytotoxicity. Solid organ transplantation is an established and useful treatment option for end-stage organ failure. Despite excellent short-term results, long-term survival of transplanted grafts has not improved accordingly because of graft rejection, graft fibrosis, or side effects of immunosuppressants. The aim of stem cell therapy for solid organ transplantation is to prevent or treat acute rejection and to involve autologous or allogeneic stem cell transplantation into patients, either through local delivery or systemic infusion. Currently, there are over 100 ongoing clinical trials to evaluate the utility of MSCs, especially in kidney transplantation [9–11].

ADSCs have been shown to consist of heterogeneous subpopulations; therefore, we hypothesized that CD90^{Hi} ADSCs might exhibit increased reprogramming capacities and subsequently have better immunoregulatory effects. Hence, the aim of the present study was to compare the reprogramming capacity of sorted murine CD90^{Hi} ADSCs. Our data demonstrated that CD90^{Hi} selection improved the reprogramming capacity of murine ADSCs, suggesting that CD90^{Hi} ADSCs could help prevent graft rejection.

2. Materials and Methods

2.1. ADSC Isolation. Murine ADSCs were isolated from B6 mice as previously described but with slight modifications [7]. Briefly, adipose tissue was obtained from the inguinal fat pads, washed with Dulbecco's phosphate-buffered saline (D-PBS; Invitrogen, Carlsbad, CA, USA) containing 50 U/mL of penicillin and 50 μg/mL of streptomycin (PSM; Invitrogen), and then cut into fine pieces, which were incubated with D-PBS containing 1.0 mg/mL of *Clostridium histolyticum* collagenase (Sigma-Aldrich, St. Louis, MO, USA) in a 37°C shaking incubator for 1 h. The digested tissue was filtered through sterile 70-μm nylon mesh, centrifuged at 430 ×g for 5 min, and resuspended in Dulbecco's modified Eagle's medium (DMEM) (Nacalai Tesque, Kyoto, Japan) supplemented with 10% fetal bovine serum (FBS; HyClone; Thermo Scientific, Waltham, MA, USA) and PSM.

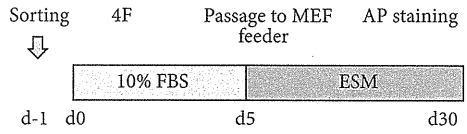

FIGURE 1: Lentiviral-mediated transfer of four iPS cell factor genes in murine ADSCs. A schematic representation of the experiment is shown. Cells were transduced with four factors (4F) after 24 h of incubation. Then, 4F-transduced cells were passaged to MMC-treated MEF feeder cells on day 5. The number of reprogrammed iPS colonies was assessed on posttransduction day 30 by AP staining.

2.2. Cell Sorting. Murine ADSCs were washed with D-PBS and treated with Accutase reagent (EMD Millipore, Billerica, MA, USA) in a 37°C incubator for 2-3 min to dissociate the cells, which were then resuspended in staining media [D-PBS supplemented with FBS (1%) and EDTA (2 mM)]. Next, the cells were stained with fluorescein isothiocyanate-conjugated anti-mouse CD34 (eBioscience, San Diego, CA, USA), phycoerythrin-conjugated anti-mouse CD31, eFluor450 anti-mouse CD45, and allophycocyanin-conjugated anti-mouse CD90.2 for 60 min at 4°C. The cells were then washed with staining media, stained with 7-aminoactinomycin D to exclude dead cells, and sorted using the FACSAria cell sorter (Bio-Rad, Hercules, CA, USA) [12]. The particular phenotypic subsets of CD90^{Hi} and CD90^{Lo} ADSCs, based on CD31, CD45, and CD90 expression, were evaluated by multicolor analysis and sorted by adequate gating.

2.3. Lentiviral Preparation. To prepare the lentiviruses, human embryonic kidney (HEK)-293Ta cells were cultured in DMEM supplemented with 10% FBS and PSM. Then, the cells were seeded at 5.0 × 10^6 cells per 100 mm dish 1 day before viral transduction. Fugene 6 transfection reagent (22.5 μL; Promega, Madison, WI, USA) was diluted with 500 μL of DMEM and incubated for 5 min at room temperature. Plasmid DNA (2.5 μg) was added to the mixture, which was incubated for an additional 15 min at room temperature. Then, the culture media was replaced with fresh DMEM supplemented 10% FBS and the DNA/Fugene 6 mixture was added dropwise onto the HEK-293Ta cells. The medium was replaced after 24 h. After an additional 48 h, virus-containing supernatants, derived from the HEK-293Ta cultures, were filtered through a 0.22-μL cellulose–acetate filter and analyzed without being frozen.

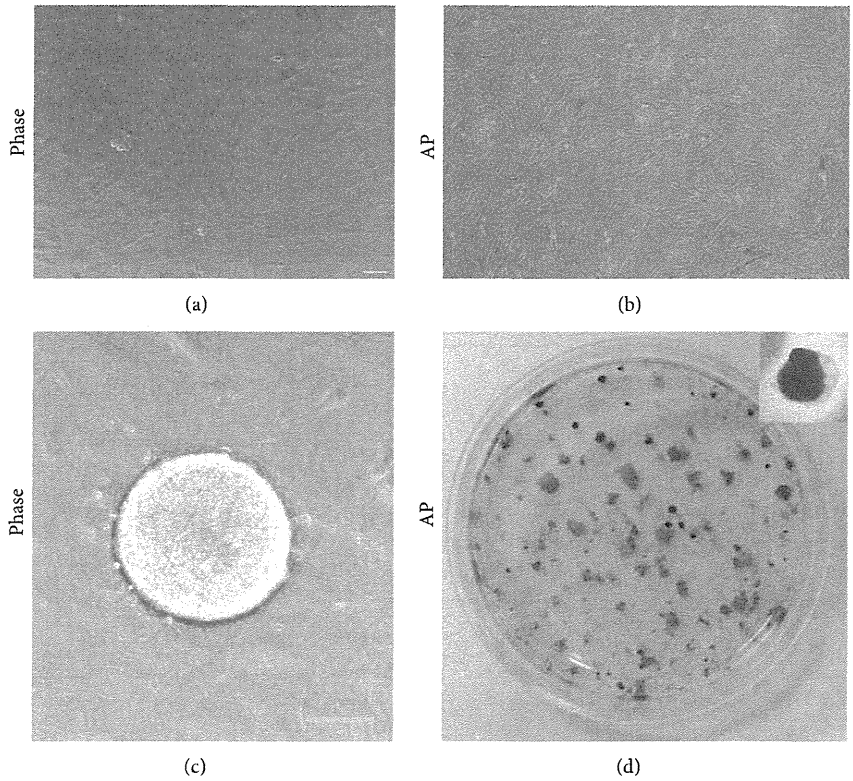

FIGURE 2: 4F transduction resulted in iPS colony formation in unsorted murine ADSCs. Phase (a and c) and AP staining (b and d) of pre- and post- (c and d) transduction were shown.

2.4. Lentiviral Transduction. Sorted $CD90^{Hi}$ and $CD90^{Lo}$ cells were plated onto 6-well culture plates at a density of 1.0×10^5 cells/well, respectively. After incubation for 24 h, the culture medium was retrieved and viral supernatants were added to each well. The next day, the cells were washed with complete medium three times. Mouse embryonic fibroblasts (MEFs) were mitotically inactivated by the addition of 10 μg/mL of mitomycin C (MMC; Nacalai Tesque Inc., Kyoto, Japan) for 90 min and then washed with D-PBS three times. The cells were then cultured with complete medium for at least 2 h, trypsinized, counted, and plated on gelatin-coated 60 mm dishes at a density of 5.0×10^5 cells/well. On posttransduction day 5, the cells were trypsinized; suspended in DMEM supplemented with 15% (v/v) FBS, PSM, 1-mM sodium pyruvate (Invitrogen), 10^{-4} M 2-mercaptoethanol (Nacalai Tesque, Inc.), nonessential amino acid solution, and 1,000 U/mL of leukemia inhibitory factor; after which they were counted. Then, 1000 cells were transferred to MMC-treated MEF feeder cells. On post-transduction day 30, alkaline phosphatase (AP) staining was performed to assess reprogramming efficiency.

2.5. AP Staining. 4F-transduced ADSCs were stained using an AP staining kit (Muto Pure Chemicals, Tokyo, Japan) following the manufacturer's recommended protocol. Briefly, cultured cells were rinsed twice with D-PBS and then fixed for 5 s in ice-cold methanol. Then, the cells were washed with tap water, stained with AP solution at 37° for 120 min, and washed again with running water. The number of AP^+ colonies were manually inspected and counted.

3. Results

Figure 1 describes the experimental protocol used in this study. First, we evaluated the reprogramming capacity of unsorted ADSCs. As shown in Figure 2, parental ADSC showed no colonies and AP staining was negative (negative control). However, 4F transduction resulted in ADSC colony formation. After culturing for 30 days, the cells were stained with AP to test iPS cell pluripotency. AP staining was positive in all colonies. These results clearly demonstrated that murine ADSCs can be reprogrammed using standard 4F. Next we used sorted ADSCs to assess the reprogramming capacities of $CD90^{Hi}$ and $CD90^{Low}$ ADSCs. As shown in Figure 3(a), the CD90 marker was widely expressed on the surfaces of the $CD31^-CD45^-CD34^-$ ADSCs. After 24 h of incubation, sorted $CD90^{Hi}$ or $CD90^{Lo}$ ADSCs became attached to the culture dishes (Figure 3(b)) and both showed similar morphologies. Next, we assessed the effect of *in vitro* culture. As shown in Figure 4(a), 7-day culture resulted in the reexpression of CD90 even after sorted $CD90^{Lo}$ ADSCs. These results suggest that sorted cells might be transduced as soon as possible.

To show the successful induction of the undifferentiated state, we employed immunocytochemistry of Oct4

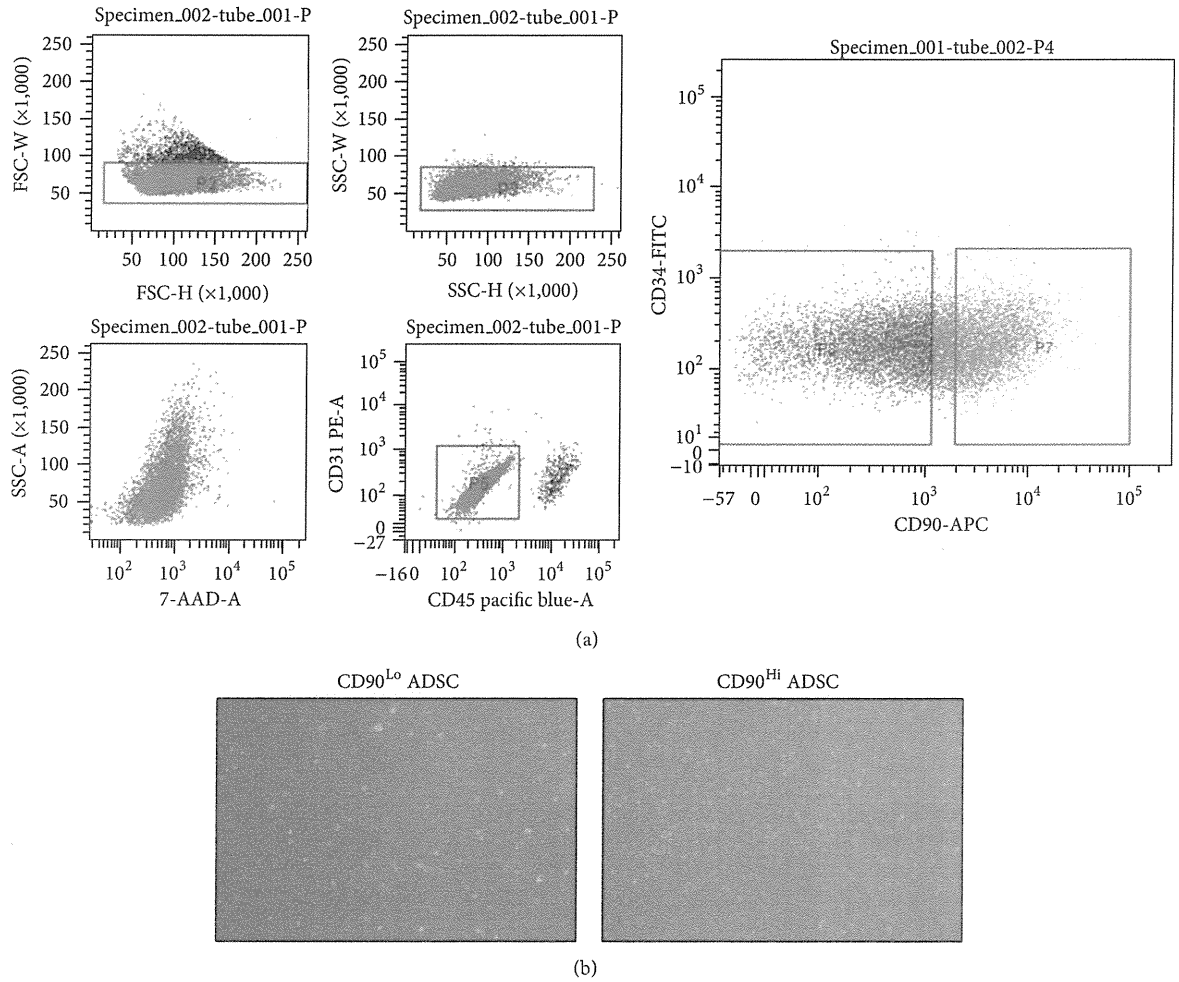

FIGURE 3: CD90^{Hi} and CD90^{Lo} sorting. (a) Gates for CD90^{Hi} (P7) and CD90^{Lo} (P8) are shown. (b) Sorted cells showed similar morphologies 24 h after sorting. Then, the cells were transduced with 4F.

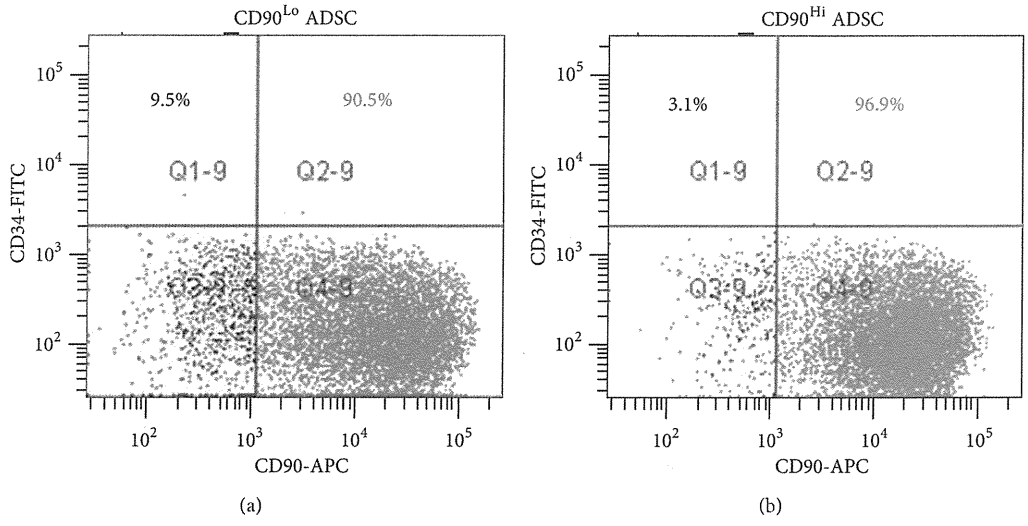

FIGURE 4: Phenotypical analysis after *in vitro* culture of sorted ADSCs.

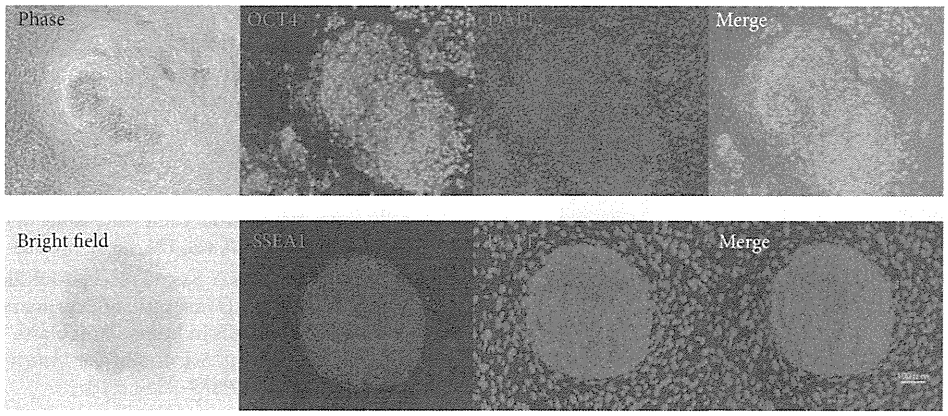

FIGURE 5: Immunocytochemistry of iPS colonies.

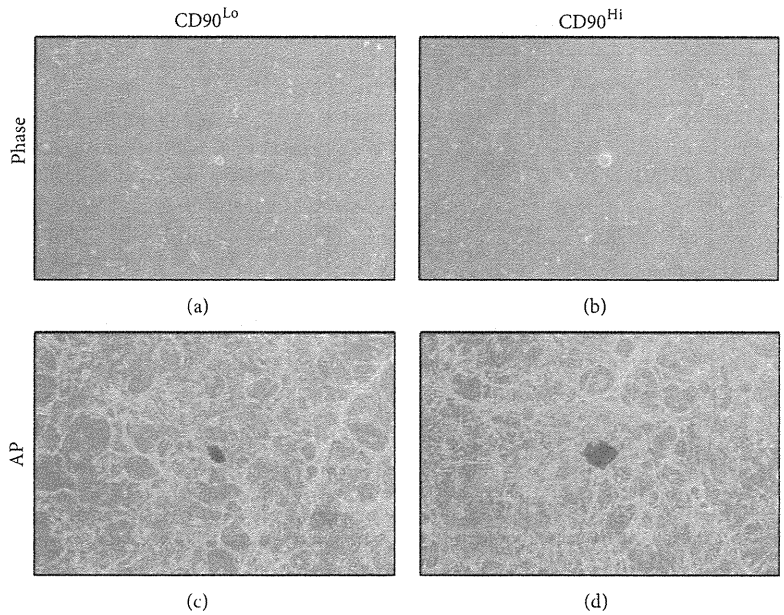

FIGURE 6: Colony formation of the sorted cells. Phase (a and b) and alkaline phosphatase staining (c and d) of $CD90^{Lo}$ (a and c) and $CD90^{Hi}$ (b and d) are shown.

and SSEA1. As shown in Figure 5, colonies were positive for Oct4 and SSEA1. Sorted and 4F-transduced ADSCs also exhibited colony formation. As shown in Figures 6(a) and 6(b), morphologically distinct colonies were visible in both $CD90^{Hi}$ and $CD90^{Lo}$ 4F-transduced ADSCs on posttransduction day 14. On posttransduction day 30, the colonies were stained with AP. There were AP+ colonies in both groups, although the $CD90^{Hi}$ ADSCs tended to form larger colonies than $CD90^{Lo}$ ADSCs (Figures 4(c) and 4(d)). As shown in Figure 7, $CD90^{Hi}$ ADSCs exhibited more AP+ colonies than $CD90^{Lo}$ ADSCs. The reprogramming efficiencies of unsorted, $CD90^{Hi}$-sorted, and $CD90^{Lo}$-sorted ADSCs were 100%, 116.5%, and 74.7%, respectively.

4. Discussion

In the present study, we demonstrated that murine ADSCs can be reprogrammed by standard 4F transduction. Furthermore, iPS cell formation was also observed in CD90-based sorted cells and the $CD90^{Hi}$ sorting resulted in enhanced reprogramming capacity of murine ADSCs compared with $CD90^{Lo}$ ADSCs with regard to colony number. Moreover, there was a trend in the association between CD90 expression level and individual colony size. These results clearly demonstrated that ADSCs have heterogeneous subpopulations and that the $CD90^{Hi}$ ADSCs present favorable candidates for the application of clinical stem cell therapy.

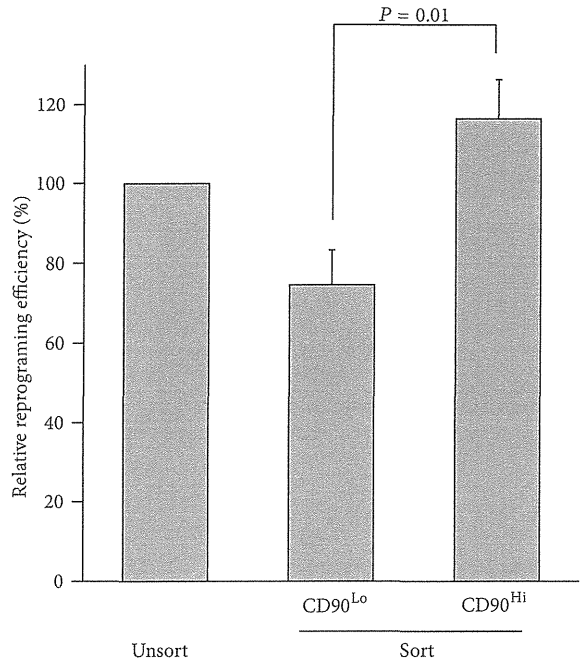

FIGURE 7: Relative reprogramming efficiency of sorted cells compared with unsorted controls.

The importance of CD90 in oncogenesis or properties of cancer stem cells has been reported [13]. CD90 expression reportedly has prognostic values in esophageal squamous cell carcinoma (ESCC) patients, because higher CD90 expression was significantly associated with a strong family history of ESCC and higher incidences of lymph node metastasis. However, the importance of CD90 expression in MSCs has not been fully elucidated; therefore, our next project is to clarify the mechanisms of CD90-mediated immunomodulatory effects. Of note, recent study reported that CD90-expressing niche stromal cells would support hematopoiesis [14].

Stem cell therapy for autoimmune disease is also well described. In a murine inflammatory bowel disease model, ADSCs alleviated experimental colitis by inhibiting inflammatory and autoimmune responses [15]. In mice, Thy-1 is also expressed by thymocytes, peripheral T cells, myoblasts, epidermal cells, and keratinocytes.

We and others previously reported that it is possible to reprogram murine and human cells to pluripotency by direct transfection of mature double-stranded microRNAs without viral vectors [16–18]. These viral-free strategies present effective methods for future stem cell therapy.

Currently, studies are underway to compare the immunoregulatory properties of viral-free strategies both *in vitro* and *in vivo*.

Acknowledgment

Lentiviral vectors (CSII-CMV-mOct3/4-IRES2-Venus, CSII-CMV-mSox2-IRES2-Venus, CSII-CMV-mKlf4-IRES2-Venus, CSII-CMV-mcMyc-IRES2-Venus, pCAG-HIVgp, and pCAG-VSV-G-RSV-Rev) were kindly provided by the Hiroyuki Miyoshi (RIKEN; The Institute of Physical and Chemical Research, Tsukuba, Japan).

References

[1] K. Takahashi and S. Yamanaka, "Induction of pluripotent stem cells from mouse embryonic and adult fibroblast cultures by defined factors," *Cell*, vol. 126, no. 4, pp. 663–676, 2006.

[2] S. Wakao, M. Kitada, Y. Kuroda et al., "Multilineage-differentiating stress-enduring (Muse) cells are a primary source of induced pluripotent stem cells in human fibroblasts," *Proceedings of the National Academy of Sciences of the United States of America*, vol. 108, no. 24, pp. 9875–9880, 2011.

[3] S. Eminli, A. Foudi, M. Stadtfeld et al., "Differentiation stage determines potential of hematopoietic cells for reprogramming into induced pluripotent stem cells," *Nature Genetics*, vol. 41, no. 9, pp. 968–976, 2009.

[4] M. T. Chung, C. Liu, J. S. Hyun et al., "CD90 (Thy-1)-positive selection enhances osteogenic capacity of human adipose-derived stromal cells," *Tissue Engineering A*, vol. 19, pp. 989–997, 2013.

[5] K. Le Blanc and D. Mougiakakos, "Multipotent mesenchymal stromal cells and the innate immune system," *Nature Reviews Immunology*, vol. 12, no. 5, pp. 383–396, 2012.

[6] M. Konno, A. Hamabe, S. Hasegawa et al., "Adipose-derived mesenchymal stem cells and regenerative medicine," *Development, Growth and Differentiation*, vol. 55, pp. 309–318, 2013.

[7] Y. Ohmura, M. Tanemura, N. Kawaguchi et al., "Combined transplantation of pancreatic islets and adipose tissue-derived stem cells enhances the survival and insulin function of islet grafts in diabetic mice," *Transplantation*, vol. 90, no. 12, pp. 1366–1373, 2010.

[8] T. Y. Yeung, K. L. Seeberger, T. Kin et al., "Human mesenchymal stem cells protect human islets from pro-inflammatory cytokines," *PLoS ONE*, vol. 7, Article ID e38189, 2012.

[9] J. Tan, W. Wu, X. Xu et al., "Induction therapy with autologous mesenchymal stem cells in living-related kidney transplants: a randomized controlled trial," *Journal of the American Medical Association*, vol. 307, no. 11, pp. 1169–1177, 2012.

[10] Y. Peng, M. Ke, L. Xu et al., "Donor-derived mesenchymal stem cells combined with low-dose tacrolimus prevent acute rejection after renal transplantation: a clinical pilot study," *Transplantation*, vol. 95, pp. 161–168, 2013.

[11] M. E. Reinders, J. W. de Fijter, H. Roelofs et al., "Autologous bone marrow-derived mesenchymal stromal cells for the treatment of allograft rejection after renal transplantation: results of a phase I study," *Stem Cells Translational Medicine*, vol. 2, pp. 107–111, 2013.

[12] S. Nishikawa, M. Konno, A. Hamabe et al., "Aldehyde dehydrogenase high gastric cancer stem cells are resistant to chemotherapy," *International Journal of Oncology*, vol. 42, pp. 1437–1442, 2013.

[13] K. H. Tang, Y. D. Dai, M. Tong et al., "A CD90(+) tumor-initiating cell population with an aggressive signature and metastatic capacity in esophageal cancer," *Cancer Research*, vol. 73, pp. 2322–2332, 2013.

[14] C. K. Chan, P. Lindau, W. Jiang et al., "Clonal precursor of bone, cartilage, and hematopoietic niche stromal cells," *Proceedings of the National Academy of Sciences of the United States of America*, vol. 110, no. 31, pp. 12643–12648, 2013.

[15] M. A. González, E. Gonzalez-Rey, L. Rico, D. Büscher, and M. Delgado, "Adipose-derived mesenchymal stem cells alleviate experimental colitis by inhibiting inflammatory and autoimmune responses," *Gastroenterology*, vol. 136, no. 3, pp. 978–989, 2009.

[16] K. Okita, M. Nakagawa, H. Hyenjong, T. Ichisaka, and S. Yamanaka, "Generation of mouse induced pluripotent stem cells without viral vectors," *Science*, vol. 322, no. 5903, pp. 949–953, 2008.

[17] N. Miyoshi, H. Ishii, H. Nagano et al., "Reprogramming of mouse and human cells to pluripotency using mature microRNAs," *Cell Stem Cell*, vol. 8, no. 6, pp. 633–638, 2011.

[18] F. Anokye-Danso, C. M. Trivedi, D. Juhr et al., "Highly efficient miRNA-mediated reprogramming of mouse and human somatic cells to pluripotency," *Cell Stem Cell*, vol. 8, no. 4, pp. 376–388, 2011.

Cell Transplantation, Vol. 22, pp. 159–173, 2013
Printed in the USA.

0963-6897/13 $90.00 + .00
DOI: http://dx.doi.org/10.3727/096368912X637028
E-ISSN 1555-3892
www.cognizantcommunication.com

Significant Improvement in Islet Yield and Survival With Modified ET-Kyoto Solution: ET-Kyoto/Neutrophil Elastase Inhibitor

Tomohiko Machida,*[1] Masahiro Tanemura,*†[1] Yoshiaki Ohmura,* Tsukasa Tanida,* Hiroshi Wada,* Shogo Kobayashi,* Shigeru Marubashi,* Hidetoshi Eguchi,* Toshinori Ito,‡ Hiroaki Nagano,* Masaki Mori,* Yuichiro Doki,* and Yoshiki Sawa§

*Department of Gastroenterological Surgery, Osaka University Graduate School of Medicine, Osaka, Japan
†Department of Surgery and Institute for Clinical Research, National Hospital Organization Kure Medical Center, Hiroshima, Japan
‡Department of Complementary and Alternative Medicine, Osaka University Graduate School of Medicine, Osaka, Japan
§Department of Cardiovascular Surgery, Osaka University Graduate School of Medicine, Osaka, Japan

Although islet transplantation can achieve insulin independence in patients with type 1 diabetes, sufficient number of islets derived from two or more donors is usually required to achieve normoglycemia. Activated neutrophils and neutrophil elastase (NE), which is released from these neutrophils, can directly cause injury in islet grafts. We hypothesized that inhibition of NE improves islet isolation and islet allograft survival. We tested our hypothesis by examining the effects of modified ET-Kyoto solution supplemented with sivelestat, a NE inhibitor (S-Kyoto solution), on islet yield and viability in islet isolation and the effect of intraperitoneally injected sivelestat on islet graft survival in a mouse allotransplant model. NE and proinflammatory cytokines such as tumor necrosis factor (TNF)-α and interleukin (IL)-6 increased markedly at the end of warm digestion during islet isolation and exhibited direct cytotoxic activity against the islets causing their apoptosis. The use of S-Kyoto solution significantly improved islet yield and viability. Furthermore, treatment with sivelestat resulted in significant prolongation of islet allograft survival in recipient mice. Furthermore, serum levels of IL-6 and TNF-α at 1 and 2 weeks posttransplantation were significantly higher in islet recipients than before transplantation. Our results indicated that NE released from activated neutrophils negatively affects islet survival and that its suppression both in vitro and in vivo improved islet yield and prolonged islet graft survival. The results suggest that inhibition of NE activity could be potentially useful in islet transplantation for patients with type 1 diabetes mellitus.

Key words: Type 1 diabetes; Islet transplantation; Neutrophil; Neutrophil elastase (NE)

INTRODUCTION

Since the reporting of the Edmonton protocol, islet transplantation has become one of the treatment options for patients with type 1 diabetes mellitus (8,41,43–48). Islet transplantation is a minimal invasive approach for β-cell replacement compared with pancreas transplantation (18,44,47). However, a sufficient number of islets derived from two or more donor pancreas are usually required to achieve insulin independence, since a substantial number of transplanted islets fail to engraft into the recipient liver for a variety of reasons such as apoptosis, inflammation, and ischemia (1,3,27,29,37,41, 42,47,52,57–59). Furthermore, research into islet transplantation has been hindered by the inability to isolate a sufficient number of islets from a single donor pancreas (4,15,16,45,47). Thus, there is a need for novel strategies that increase islet yield, maintain high islet quality, and protect transplanted islet grafts.

Indeed, the islet isolation procedure itself can lead to tissue destruction and activation of cellular and noncellular components of the pancreas, including resident neutrophils, macrophages, and T cells, which probably play an important role in impairment of islet survival (1,4,31,37,42). In the present study, we focused on the role of neutrophils, in particular neutrophil elastase (NE), against islets during islet isolation. The NE is a 29-kDa (kilodalton) glycoprotein chymotrypsin-like serine protease stored in azurophil granules in its inactive form until it is released after neutrophil exposure to inflammatory stimuli (17,49,55). Once released, NE is fully

Received June 17, 2011; final acceptance January 10, 2012. Online prepub date: April 2, 2012.
[1]These authors provided equal contribution to this work.
Address correspondence to Masahiro Tanemura, M.D., Ph.D., Department of Gastroenterological Surgery, Osaka University Graduate School of Medicine, 2-2 Yamadaoka, Suita, Osaka 565-0871, Japan. Tel: +81-6-6879-3251; Fax: +81-6-6879-3259; E-mail: mtanemura@gesurg.med.osaka-u.ac.jp

active, and the excessive release of NE degrades elastin, collagens, laminins, and other extracellular matrix components, thereby leading to subsequent tissue damage through endothelial cell injury (12,17,49,54,55).

Sivelestat (ONO-5046) is a low molecular weight synthetic specific and competitive inhibitor of NE activity (12,17,21,30,49,50,54,55,60). This agent has been employed clinically in Japan and shown to attenuate acute lung injury associated with systemic inflammation response, which is sometimes seen after infection, surgical intervention, traumatic, or burn injury (11,49,50,60). In addition, sivelestat exhibits potent cytoprotective properties in animal models of liver and lung transplantation (30,54), hepatectomy (17,21), and ischemia/reperfusion injury (17,54,55).

The objectives of the present study were to determine whether the addition of sivelestat to the islet isolation solution improves islet yield and viability. We also investigated the cytoprotective effects of sivelestat in islet recipients. The results suggested that NE inhibition using sivelestat is an attractive new therapeutic option in islet isolation and transplantation and could have a significant impact on patients with type 1 diabetes by allowing successful one donor to one recipient.

MATERIALS AND METHODS

Drugs and Reagents

Sivelestat (ONO-5046) is a newly synthesized agent known to selectively inhibit NE. Sivelestat was a generous gift from Ono Pharmaceutical Co., Ltd. (Osaka, Japan). A stock solution was prepared by dissolving 200 mg of sivelestat at room temperature in 20 ml of phosphate-buffered saline (PBS) with 24.5 mg of sodium carbonate and stored at 4°C until use.

Preservation Solutions

University of Wisconsin (UW, Bristol-Myers Squibb Company, Princeton, NJ) and extracellular-type trehalose-containing Kyoto (ET-Kyoto; Otsuka Pharmaceutical, Tokyo, Japan) solution were prepared. Stock solutions of 20 μM sivelestat in UW and ET-Kyoto were prepared as S-UW, S-Kyoto, each. Sivelestat did not change the density of islets or other tissue components of the pancreas.

Mice

Male C57BL/6J mice and Balb c/A mice, 10–12 weeks old, weighting 20–30 g, were purchased from CLEA Japan, Inc. (Tokyo). All experiments were approved by the international animal care and use committee (IACUC) of Osaka University Medical School.

Islet Isolation and Assessment

Briefly, after clamping the distal common bile duct under anesthesia, the common bile duct was cannulated. Then the pancreatic tissue was distended by using 3 ml of isolation solution containing 1 mg/ml of collagenase VIII (Sigma-Aldrich; USA). The distended pancreas was excised and incubated in 37°C warm shaker for 15 min. The digested pancreas was washed with appropriate isolation solution three times by centrifugation (270×*g*, 2 min, 4°C), then purified with a discontinuous density gradient (1.111, 1.104, 1.097, 1.072 g/ml) in isolation solution containing iodixianol (Optiplep®, Axis-Shild, Oslo, Norway). The purified islets were collected and cultured with Roswell Park Memorial Institute (RPMI) 1640 medium (Sigma-Aldrich) supplemented with 10% fetal bovine serum (FBS) (Sigma-Aldrich), 100 U/ml penicillin, 100 μg/ml streptomycin, and 0.1 mM non-essential amino acids (Invitrogen, Carlsbad, CA) under 5% CO_2 atmosphere at 37°C (26).

To evaluate the isolated islets, islet count, islet equivalents (IEQ), distribution of islet size, and islet purity were determined as described previously (35,40). Islet yield and distribution of islet size were determined by measuring islets after dithizone staining (Wako, Osaka) using VH analyzer (Keyence, Osaka). The purification recovery rate was defined as the percentage of IEQ recovered after purification compared to the IEQ before purification (34). Islet purity was assessed by four independent investigators.

In Vitro Cytotoxicity Assay

The cytotoxic activity of NE against isolated islets was assessed by the lactate dehydrogenase (LDH) assay kit (Roche Applied Science, Mannheim, Germany). Briefly, the harvested islets were plated at 30 islets/well in 96-well round plate. NE (Calbiochem, San Diego, CA) was then added to the wells at various concentrations, and the plates were incubated for 24 h at 37°C. Next, 100 μl of the culture supernatant was transferred into the wells of 96-well flat plate. The reaction mixture was added to each well, and then absorbance was measured at 490 nm. Moreover, to examine the cytoprotective effects of sivelestat on NE cytotoxicity, 2, 20, or 200 μM of sivelestat was simultaneously added to the NE-containing wells and the plates were incubated for 24 h at 37°C followed by measurement of absorbance at 490 nm.

Staining for Naphthol AS-D Chloroacetate Esterase

To assess the accumulation of activated neutrophils in the pancreas during islet isolation, the tissue was stained by naphthol AS-D chloroacetate esterase (Sigma-Aldrich) as described previously (14,17). Briefly, the pancreas specimens obtained before and at the end of warm digestion were fixed in 10% formalin and embedded in paraffin. Tissue sections (2-μm thick) were stained with naphthol AS-D chloroacetate esterase. In addition, the specimens were counterstained with hematoxylin. Activated

neutrophils were positively stained red-brown and counted under the microscope at a magnification of 100×.

Neutrophil Elastase Activity Assay

NE enzyme activity was measured in the supernatant at each step of islet isolation, including before warm digestion, at the end of warm digestion, and after purification, using the method described previously (11,12,17, 55,59). For this purpose a 20-µl sample was incubated with 1 mM of *N*-methoxysuccinyl-Ala-Ala-Pro-Val-*p*-nitroanilide (*p*-NA) (Sigma-Aldrich), which is a highly specific synthetic substrate for NE, in 0.1 M Tris–HCl buffer (pH 8.0) containing 0.5 M NaCl at 37°C for 24 h. The incubated samples were plated onto a 96-well plate, and then absorbance was measured at 405 nm to detect free *p*-NA.

Assessment of Apoptosis of Isolated Islets

Terminal deoxynucleotidyl transferase dUTP nick-end labeling (TUNEL) staining was performed to detect apoptotic cells during islet isolation, using Apop Tag® Peroxidase In Situ Apoptosis Detection Kit (Chemicon International, Temecula, CA) as described previously (53–55). The negative control was prepared by omission of the terminal transferase. Positive control was generated by treatment with deoxyribonuclease (DNase) I. Peroxidase activity was visualized with diaminobenzidine (DAB) substrate, which yielded a brown oxidation product, and 0.5% methyl green was used for counterstaining. TUNEL-positive cells were counted under the microscope at 400× magnification.

Scanning Electron Microscopy (SEM)

Morphological analysis of the isolated islets was carried out by SEM as described previously (31). The isolated islets were fixed with 2.5% PBS (0.1 M, pH 7.4) glutaraldehyde (Tokyo Chemical Industry, Tokyo) solution at 4°C for 24 h. After washing, they were postfixed with 1% OsO_4/PBS for 2 h at 4°C. Subsequently, the fixed islets were incubated in 1% tannin acid solution at 4°C overnight and then dehydrated. They were transferred to isoamyl acetate and dried in a critical point dryer using liquid CO_2. They were mounted on the stage and observed under a scanning electron microscope (S-800, Hitachi, Tokyo). The morphology was assessed by four independent investigators.

Islet Viability Assay

The viability of isolated islets was assessed by tetramethyl rhodamine ethyl ester (TMRE; Molecular Probes, Eugene, OR) assay and 7-aminoactinomycin D (7-AAD; Molecular Probes) assay, as described previously (9). TMRE is an indicator of the mitochondria membrane potential (MMP) and used as a marker for live cells, while 7-AAD is used as a marker for dead cells or apoptotic cells. Briefly, the isolated islets were cultured for 24 h and then incubated in 1 ml of TrypLE Express (Invitrogen) for 15 min at 37°C to prepare single islet cells and then dispersed. The single islet cells were incubated with 100 ng/ml of TMRE for 30 min at 4°C. Subsequently, the fluorescence intensity of TMRE was analyzed with a FACS Calibur flow cytometer (BD Immunocytometry, San Jose, CA). In a similar fashion, the isolated islets were dispersed into single cells and then incubated with 1 µg/ml of 7-AAD. Subsequently, the fluorescence intensity of 7-AAD was analyzed with a FACS Calibur flow cytometer.

To further determine the islets viability, the colorimetric methyl tetrazolium salt (MTS) assay was performed as described previously (56). The viability of freshly isolated islets or cultured islets over either 24 or 48 h was evaluated by monitoring metabolic activity with MTS assay using the cell Titer 96 Aqueous One reagent (Promega, Madison, WI). The colorimetric reagent was added to each well and incubated for 2 h, and the absorbance values were read at 490 nm.

Glucose-Stimulated Insulin Release In Vitro

To evaluate the in vitro insulin function of islets, static glucose change was measured as described previously (33,35). Twenty islets were cultured overnight at 37°C and then preincubated in low-glucose culture medium (2.8 mM glucose) for 60 min at 37°C. After preincubation, the islets were incubated in low-glucose culture medium (2.8 mM glucose) at 37°C for 60 min. Subsequently, the supernatant of the culture medium was collected, and the islets were incubated in high-glucose culture medium (20 mM glucose) at 37°C for 60 min. Similarly, the supernatant was collected, and insulin concentration was measured by the mouse-insulin enzyme-linked immunosorbent assay (ELISA) kit (Mercodia, Uppsala, Sweden). Glucose-stimulated insulin concentration was expressed as the stimulation index (SI), calculated as the ratio of insulin released during exposure to high glucose over the insulin released during low-glucose incubation.

Islet Transplant Experiments

The recipient 10- to 12-week-old male Balb c/A mice were divided at random into two experimental groups (Fig. 6A) ($n = 5$/group) to receive allogeneic islets isolated from C57BL/6J mice by the use of either isolation solution (i.e., ET-Kyoto and S-Kyoto solutions). The recipient mice were rendered diabetic by a single injection of streptozotocin (STZ) (Nacalai tesque, Kyoto, Japan) at a dose of 180 mg/kg intraperitoneally. Hyperglycemia was defined as glucose level of >400 mg/dl measured twice consecutively after STZ injection. Then 500 of freshly isolated islets were transplanted under the kidney

capsule. After transplantation, nonfasting blood glucose level was monitored using samples from tail blood by Glutest PRO (Sanwa kagaku, Nagoya, Japan). Normoglycemia after transplantation was defined as two consecutive blood glucose levels below 200 mg/dl. Islet rejection after transplantation was defined when two consecutive blood glucose levels exceeded 200 mg/dl. At 1 week posttransplantation, the engrafted kidneys were excised to assess the survival of islet grafts by immunohistochemistry. Moreover, the beneficial effects of monotherapy with intraperitoneal sivelestat in recipient mice were assessed. Sivelestat was administered at 100 mg/kg/day for 1 day before transplantation and every day until 14 days after transplantation, as described previously (32). The recipient Balb c/A mice treated with sivelestat were divided at random into two experimental groups ($n=5$/group) to receive allogeneic islets isolated from C57BL/6J mice using ET-Kyoto or S-Kyoto solution.

Intraperitoneal Glucose Tolerance Test (IPGTT)

The IPGTT was performed at 1 week posttransplantation, using the method described previously (2,9,58). Mice ($n=3$/group) were fasted overnight and then injected intraperitoneally (IP) with 2 g glucose in saline/kg body weight. Untreated diabetic mice and nondiabetic wild-type mice were transplanted with saline as a control. Blood glucose levels were measured before injection and at 15, 60, and 120 min after injection.

Immunohistochemical Analysis

Immunohistochemical analysis was performed using the method described previously (36). The engrafted kidneys were excised, fixed in formalin, and embedded in paraffin. Tissue sections (2-μm thick) were placed in 0.3% H_2O_2/methanol to quench endogenous peroxidase activity and incubated with 5% bovine serum albumin (BSA)-PBS to block nonspecific reaction. The slides were incubated with rabbit anti-insulin polyclonal antibody (pAb, Santa Cruz Biotechnology, CA) to detect the transplanted islets. The sections were incubated with horseradish peroxidase (HRP)-conjugated secondary antibody (Bethyl Laboratories, Inc., Montgomery, TX) and then immunostaining was visualized with 0.02% DAB (Sigma-Aldrich) as the chromogen. After washing, the sections were counterstained with hematoxylin. Control tissue sections were prepared in a similar fashion, except no primary antibody was used.

Measurement of Proinflammatory Cytokines

The supernatant was collected after each step of islet isolation, including before warm digestion, at the end of warm digestion and after purification. Moreover, serum samples were collected from islet recipients at day 1 before transplantation and days 4, 7, 14, 21, 28 after transplantation. These samples were frozen immediately at −80°C until analysis. Proinflammatory cytokine (IL-2, IL-4, IL-6, IL-10, IL-17A, IFN-γ, TNF-α) levels in these samples were measured using the BD™ Cytometric Bead Array Mouse Th1/Th2/Th17 CBA kit (BD Biosciences, San Jose, CA) and analyzed on a FACS Calibur Flow cytometer (BD Immunocytometry).

Statistical Analysis

Values were expressed as mean ± SD. Differences between groups were examined for statistical significance using the two-tailed unpaired Student's t test or one-way analysis of the variance (ANOVA) followed by Bonferroni's post hoc test when multiple comparisons were made. A value of $p<0.05$ denoted the presence of significant difference.

RESULTS

Direct Cytotoxicity of Neutrophil Elastase and Optimum Effective Concentration of Sivelestat

To assess the direct cytotoxicity of NE against isolated islets, LDH assay was performed at various concentrations of this enzyme. NE caused 43–48% killing at both 5 and 10 μg/ml. To prevent this killing, sivelestat was added to the culture medium at 2, 20, or 200 μM. The cytotoxicity induced by 10 μg/ml of NE could not be inhibited by sivelestat (Fig. 1A). However, the cytotoxicity induced by less than 5 μg/ml of NE was significantly abrogated by either 20 or 200 μM of sivelestat, but not by 2 μM of sivelestat (Fig. 1A).

To elect the optimum concentration of sivelestat for islet isolation, islet isolation was performed by the addition of various concentrations of sivelestat to the isolation solution (Fig. 1B). Islet yields using a high concentration of sivelestat (200 μM or 2 mM) were significantly lower than that with 20 μM of sivelestat. In contrast, no significant improvement in islet yield was observed by 2 μM of sivelestat isolation compared with that of the control group (ET-Kyoto isolation). These findings correlated with those from LDH assay, and thus, the following experiments were performed using 20 μM of sivelestat.

Activation of Neutrophils in Pancreas During Collagenase Digestion

Naphthol AS-D chloroacetate esterase staining was performed to demonstrate whether resident neutrophils in the pancreas tissue are activated by collagenase digestion. Many neutrophils were activated (red-brown staining) by collagenase digestion in islet isolation using both UW and ET-Kyoto solutions (Fig. 2A), but their number (cells/field) was significantly reduced by the addition of 20 μM of sivelestat in ET-Kyoto solution (UW: 10.2 ± 1.1, S-UW: 6.8 ± 0.4, ET-Kyoto: 9.2 ± 1.3, S-Kyoto: 3.6 ± 0.5) (UW, ET-Kyoto vs. S-Kyoto: $p<0.001$, S-UW vs. S-Kyoto:

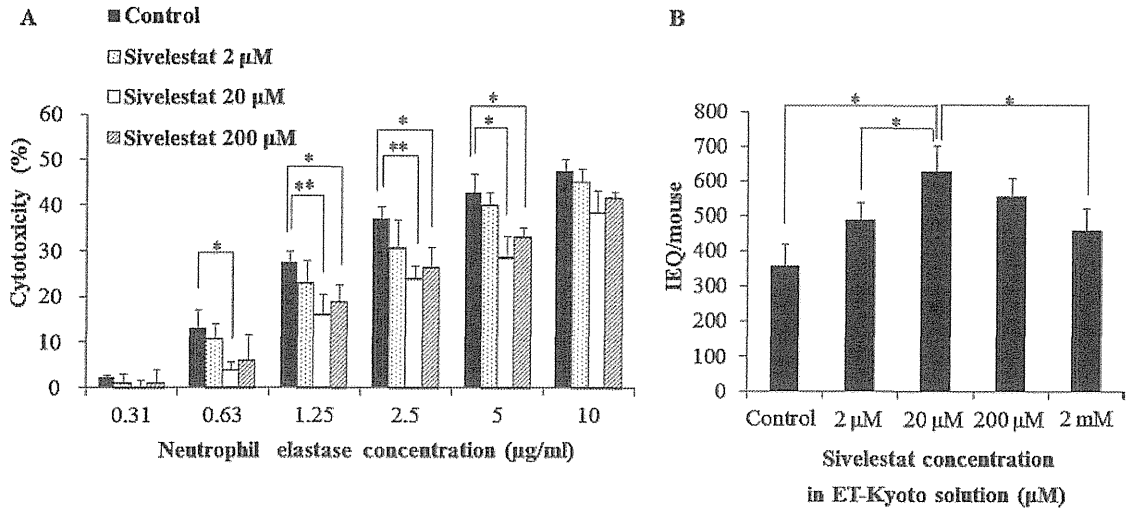

Figure 1. In vitro cytotoxicity assay of neutrophil elastase against islets and optimum concentration of sivelestat in ET-Kyoto solution. (A) The cytotoxicity of neutrophil elastase against islets and the inhibitory effects of sivelestat were assessed by lactate dehydrogenase (LDH) assay. Data are mean ± SD of three independent experiments; $*p<0.05$, $**p<0.01$. (B) Islet yields under various concentrations of sivelestat. Data are mean ± SD of three independent experiments; $*p<0.05$.

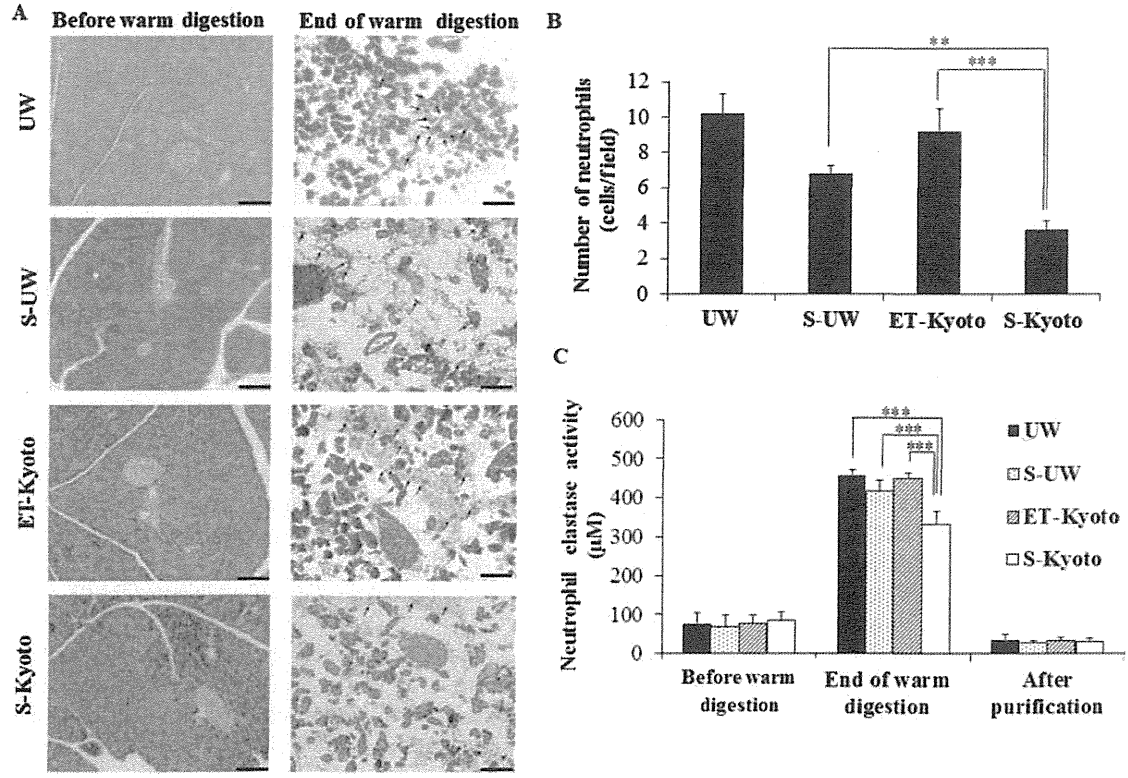

Figure 2. Accumulation of activated neutrophils in the pancreas and neutrophil elastase activity during islet isolation. (A) Representative histology of the pancreas before and at the end of warm digestion. Activated neutrophils are stained red-brown (black arrow) by naphthol AS-D chloroacetate esterase. Scale bars: 100 μm. (B) Number of activated neutrophils per field (original magnification: 100×) was counted under microscopy. Data are mean ± SD of five sections; $**p<0.01$, $***p<0.001$. (C) Neutrophil elastase activity in the supernatant during islet isolation measured at various time points of islet isolation (before warm digestion, at the end of warm digestion, after purification). Data are mean ± SD of five independent samples; $***p<0.001$. UW, University of Wisconsin solution.

$p<0.01$) (Fig. 2B). These results suggest a marked increase in enzyme activity by collagenase digestion in all types of isolation solutions (Fig. 2C). However, the enzyme activity was significantly suppressed in S-Kyoto islet isolation than those in other isolations (UW, S-UW, and ET-Kyoto isolation).

Sivelestat Suppresses Apoptosis in Islets After Warm Digestion During Islet Isolation

Many TUNEL-positive cells were identified in the islets at the end of warm digestion (Fig. 3A), whereas no such cells were detected before digestion (data not shown). Quantitative analysis indicated a significantly lower number of TUNEL-positive cells within the islets of the S-Kyoto group (6.6±1.5) compared with those of UW, S-UW, and ET-Kyoto groups (23.1±3.9, 20.8±5.0, and 15.3±2.6, respectively) ($p<0.001$, each) (Fig. 3B).

Improvement of Islet Yield Elicited by Islet Isolation With S-Kyoto Solution

To investigate the beneficial effects of sivelestat in islet isolation, islet isolations were performed using either UW or ET-Kyoto solution, with or without 20 μM of sivelestat. Islet yield, isolation index, and islet purity after purification were significantly improved by S-Kyoto islet isolation (Table 1). The recovery rate of purification was also significantly improved by S-Kyoto islet isolation, compared to those by other isolation solutions (UW: 55.8±10.4%, S-UW: 56.6±12.7%, ET-Kyoto: 56.6±4.6%, S-Kyoto: 76.0±5.2%). Based on the results of UW isolation groups (UW, S-UW), no beneficial effects of sivelestat were elicited under these islet isolation parameters. With regard to islet size distribution, the percentage of large islets (>150 nm in diameter) in the S-Kyoto group was markedly higher than that in other isolation groups (Fig. 4A).

To further examine the morphological changes in isolated islets, SEM was employed. As shown in Figure 4B, islets obtained from the UW groups (UW, S-UW) were poor, based on the irregular islet surface and detection of islet damage during the isolation procedure. Similarly, islets obtained from ET-Kyoto isolation had irregular shape. On the other hand, islets isolated by S-Kyoto solution were well preserved, with round and smooth surface.

Improvement of Islet Viability Elicited by Islet Isolation With S-Kyoto Solution

Next, we evaluated islet viability using fluorescence labeling with TMRE and 7-AAD (Fig. 5). In the UW groups (UW, S-UW), no significant difference was noted in islet viability assay using TMRE and 7-AAD between with or without sivelestat [UW ($n=5$) vs. S-UW ($n=5$) (60.0±5.6% vs. 63.3±4.4%, not significant)]. However,

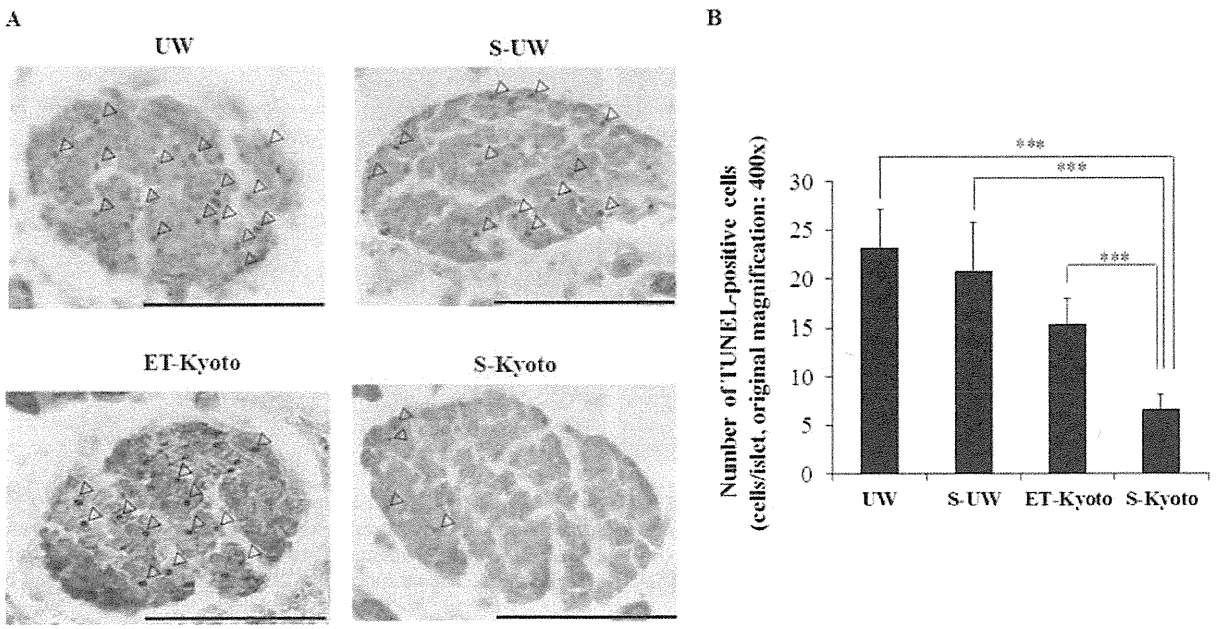

Figure 3. Assessment of apoptosis during islet isolation by TUNEL staining. (A) Representative histological sections of the islets at the end of warm digestion. Note the brown terminal deoxynucleotidyl transferase dUTP nick-end labeling (TUNEL)-stained apoptotic cells (arrowhead). Scale bars: 100 μm. (B) The density of TUNEL-positive cells (cells/islet) was determined under magnification of 400×. All experiments were done using each independent mouse. One mouse was used in each experiment ($n=1$). Data are mean±SD of five independent sections; ***$p<0.001$.

Table 1. Results of Islet Isolation According to the Isolation Solution

	UW	S-UW	ET-Kyoto	S-Kyoto
Islet count after purification (cells/mouse)	248±92*	270±121	280±86	332±74
IEQ after purification	243±68§	276±126¶	367±70*	651±52
Recovery rate of purification	55.8±10.4¶	56.6±12.7*	56.6±4.6*	76.0±5.2
Isolation index	1.18±0.21§	1.20±0.38¶	1.56±0.21*	2.05±0.17
Islet purity (%)	82.7±3.1§	84.0±2.2¶	87.3±2.7	91.3±1.9

Data are expressed as mean±SD of five independent experiments. *$p<0.05$, ¶$p<0.01$, §$p<0.001$, compared with S-Kyoto isolation solution. Islet count and purity were measured by the VH analyzer software. Isolation index was calculated as the ratio of IEQ to islet count. The recovery rate of purification (%)=IEQ after purification/IEQ before purification×100. IEQ, islet equivalents; UW, University of Wisconsin.

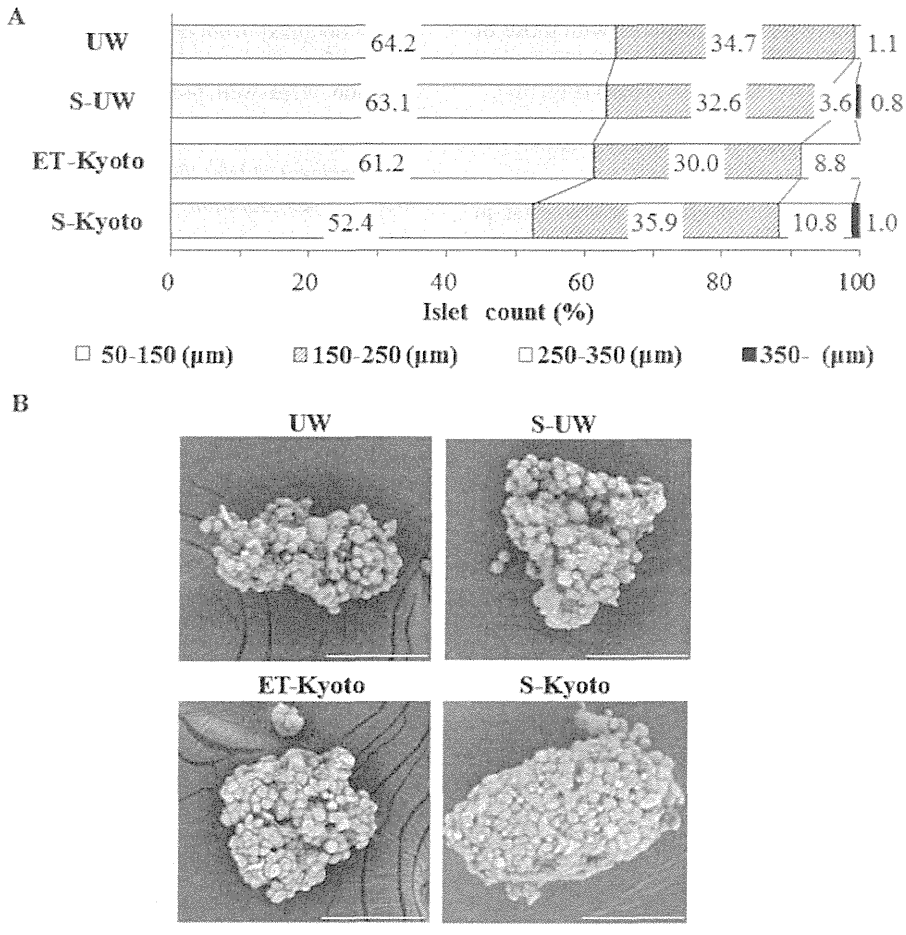

Figure 4. Results of islet isolation according to the type of isolation solution. (A) Size distribution for each diameter (50–150, 150–250, 250–350, 350– μm) of isolated islets assessed by using each isolation solution. All experiments were done using each independent mouse. One mouse was used in each experiment ($n=1$). Data are the mean percentage from five independent experiments. (B) Representative microscopic images of the islets immediately after isolation. The morphology of isolated islets was observed by scanning electron microscopy. Scale bars: 100 μm.

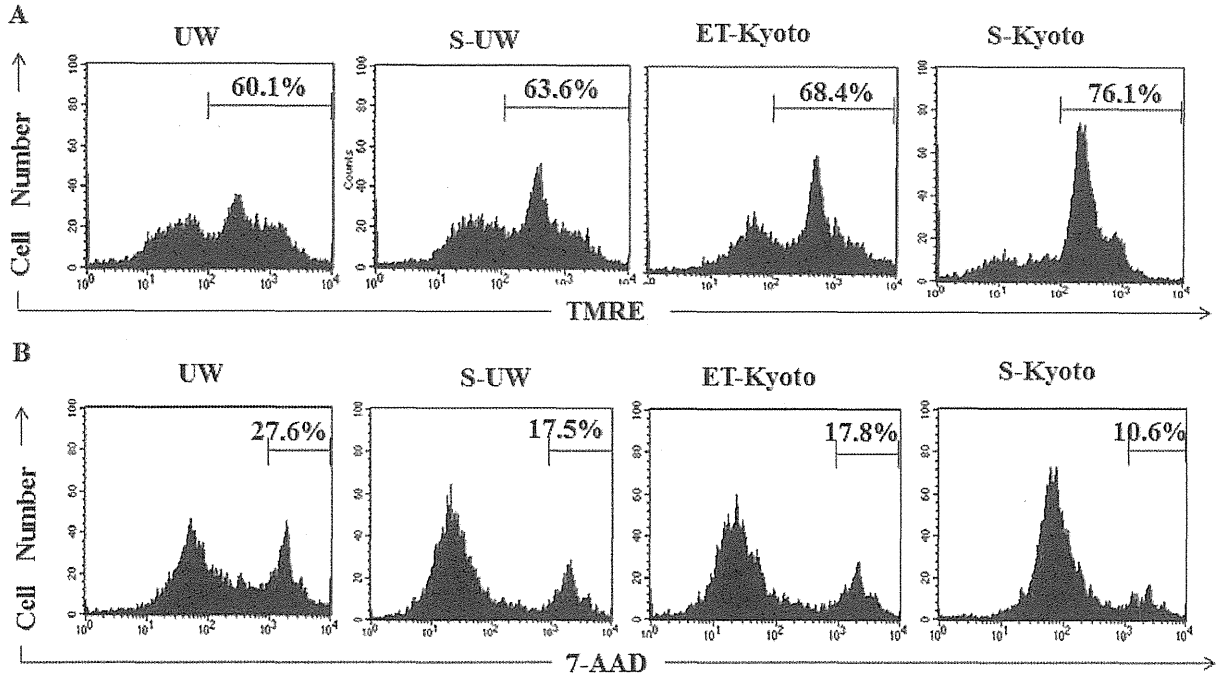

Figure 5. In vitro viability assay of isolated islets by TMRE and 7-AAD. (A) Representative flow cytometry analysis by tetramethyl rhodamine ethyl ester (TMRE) assay. (B) Representative flow cytometry analysis by 7-aminoactinomycin D (7-AAD). Percentage data represent percentages of cells with high fluorescence.

the percentage of dead cells, represented by 7-AAD-positive cells, was significantly reduced in S-UW isolation group [UW ($n=5$) vs. S-UW ($n=5$), 25.8±5.3% vs. 17.2±1.3%, $p<0.05$]. In contrast, the viability of islets isolated with S-Kyoto solution was significantly better relative to that of ET-Kyoto isolation [ET-Kyoto ($n=5$) vs. S-Kyoto ($n=5$), 67.0±1.2% vs. 75.4±2.0%, $p<0.001$]. Moreover, the percentage of dead cells in the S-Kyoto group was also lower compared with that in ET-Kyoto isolation [ET-Kyoto ($n=5$) vs. S-Kyoto ($n=5$), 18.6±2.2% vs. 11.6±2.4%, $p<0.01$]. Similar findings of islet viability were noted by MTS assay (Fig. 6A). The highest viability of fresh islets was noted with S-Kyoto solution [ET-Kyoto ($n=5$) vs. S-Kyoto ($n=5$), 0.172±0.013 vs. 0.206±0.026, $p<0.05$] (Fig. 6A). With regard to the in vitro culture after islet isolation, although islet viability in each group decreased gradually, that of the S-Kyoto group was well preserved compared with other isolation groups (Fig. 6B).

Improvement of Islet Function Elicited by Islet Isolation With S-Kyoto Solution

Next, we evaluated insulin function of islets using static glucose change. Although no significant difference was observed in insulin concentration under low glucose (2.8 mM) using each solution, insulin concentration under high glucose (20 mM) and the SI improved significantly by S-Kyoto islet isolation in comparison with those of other isolation solutions (Table 2). Based on the results of UW isolation groups (UW, S-UW), no beneficial effects of sivelestat were elicited as determined by the SI.

Prolongation of Islet Graft Survival in S-Kyoto Group and in In Vivo Experiments

Transplantation of 500 allogeneic islets of the ET-Kyoto group was associated with graft survival of 7.4±1.1 days (Fig. 7A, Table 3). A significant prolongation of islet graft survival was noted after transplantation of the S-Kyoto group, compared with islet grafts of the ET-Kyoto group (11.2±1.3 days, $p<0.05$). Importantly, islet transplantation coupled with 15-day intraperitoneal administration of 2 mg/day sivelestat elicited significant prolongation of graft survival, compared with both ET-Kyoto and S-Kyoto groups, respectively (Fig. 7A, Table 3). Next, NE activity in sera of recipient mice was measured. NE activity increased gradually after islet transplantation in the S-Kyoto group. However, sivelestat significantly suppressed the enzyme activity measured at day 28 after transplantation (Fig. 7B). These results suggest that prolongation of islet graft survival in the sivelestat IP group is due to inhibition of NE enzyme activity and the anti-inflammatory properties of sivelestat.

To examine islet graft function in vivo, IPGTT was performed at day 7 after transplantation. In nondiabetic

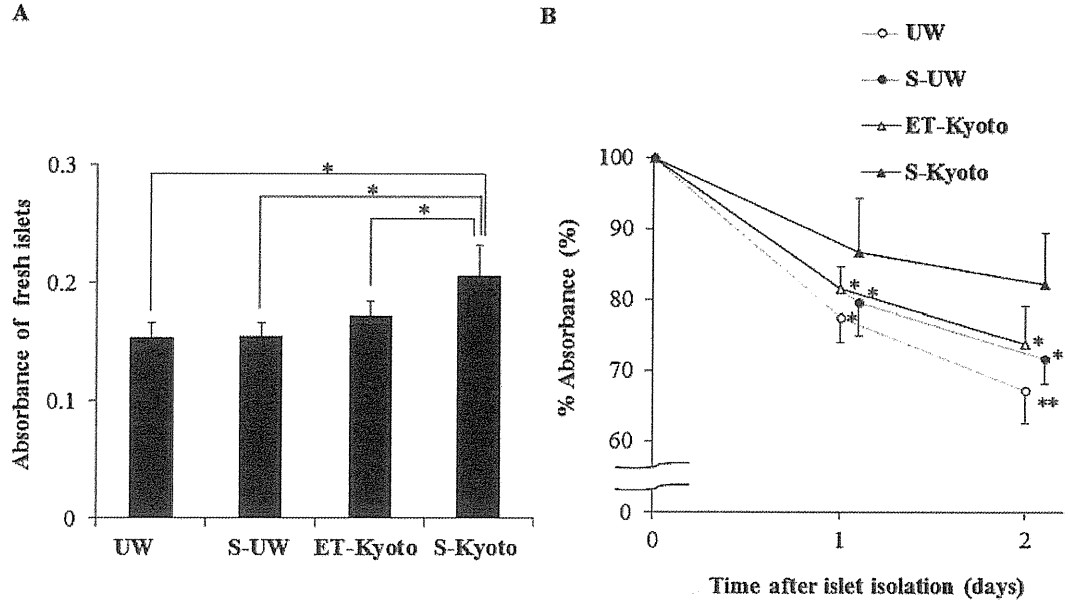

Figure 6. In vitro viability assay of isolated islets by MTS. (A) Viability of fresh islets (30 islets) was assessed using MTS assay. Data are mean ± SD of five independent experiments; $*p<0.05$. (B) Isolated islets (30 islets) were cultured for 0, 1, 2 days, and their viabilities were assessed by MTS assay. Data are mean ± SD of five independent experiments; $*p<0.05$, $**p<0.01$ versus fresh islets.

wild-type mice, injection of glucose-induced hyperglycemia with the peak blood glucose level recorded at 15 min, but the level returned to normal at 60–120 min after the injection (Fig. 7C). A similar pattern was observed in mice transplanted with S-Kyoto and S-Kyoto and treated with sivelestat. On the other hand, blood glucose levels of mice transplanted with ET-Kyoto group and untreated diabetic mice were significantly higher than those of the control wild-type mice before injection and at 15, 60, and 120 min after injection of glucose (Fig. 7C). Immunohistochemical staining for insulin confirmed that islet transplantation with S-Kyoto and S-Kyoto with sivelestat prolonged graft survival. Small islet grafts with many infiltrating inflammatory cells were detected at day 7 after transplantation in the ET-Kyoto group, whereas insulin-positive islet grafts with well preserved islet structure were found in the S-Kyoto and S-Kyoto with sivelestat groups (Fig. 7D).

Sivelestat Suppresses Proinflammatory Cytokines After Warm Digestion During Islet Isolation

We measured the levels of proinflammatory cytokines (IL-2, IL-4, IL-6, IL-10, IL-17A, IFN-γ, TNF-α) in the isolation solution at each step of islet isolation, including before warm digestion, at the end of warm digestion, and after purification. The levels at the end of warm digestion were markedly higher than before warm digestion (Fig. 8). On the other hand, IL-6 and TNF-α levels were significantly lower at the end of warm digestion in S-Kyoto solution compared with other isolation solutions such as UW and ET-Kyoto (Fig. 8).

Sivelestat Suppresses Proinflammatory Cytokines in Serum of Islet Recipients After Transplantation

The serum levels of IL-6 and TNF-α in islet recipients were significantly higher at 7 and 14 posttransplantation days than before transplantation (day −1), whereas no

Table 2. Insulin Concentration Under Low (2.8 mM) and High (20 mM) Glucose and Stimulation Index According to the Isolation Solution Used in the Present Study

	UW	S-UW	ET-Kyoto	S-Kyoto
Insulin concentration (μg/L) under:				
Low glucose (2.8 mM)	2.89 ± 0.37	2.75 ± 0.44	2.90 ± 0.30	2.98 ± 0.37
High glucose (20 mM)	3.68 ± 0.52¶	3.64 ± 0.54¶	3.78 ± 0.44¶	4.46 ± 0.79
Stimulation index (SI)	1.30 ± 0.06§	1.31 ± 0.12§	1.38 ± 0.12*	1.49 ± 0.08

Data are expressed as mean ± SD of five independent experiments. $*p<0.05$, $¶p<0.01$, $§p<0.001$, compared with the S-Kyoto solution. SI was calculated as the ratio of insulin released during exposure to high glucose over the insulin released during low glucose incubation. SI, stimulation index; UW, University of Wisconsin.

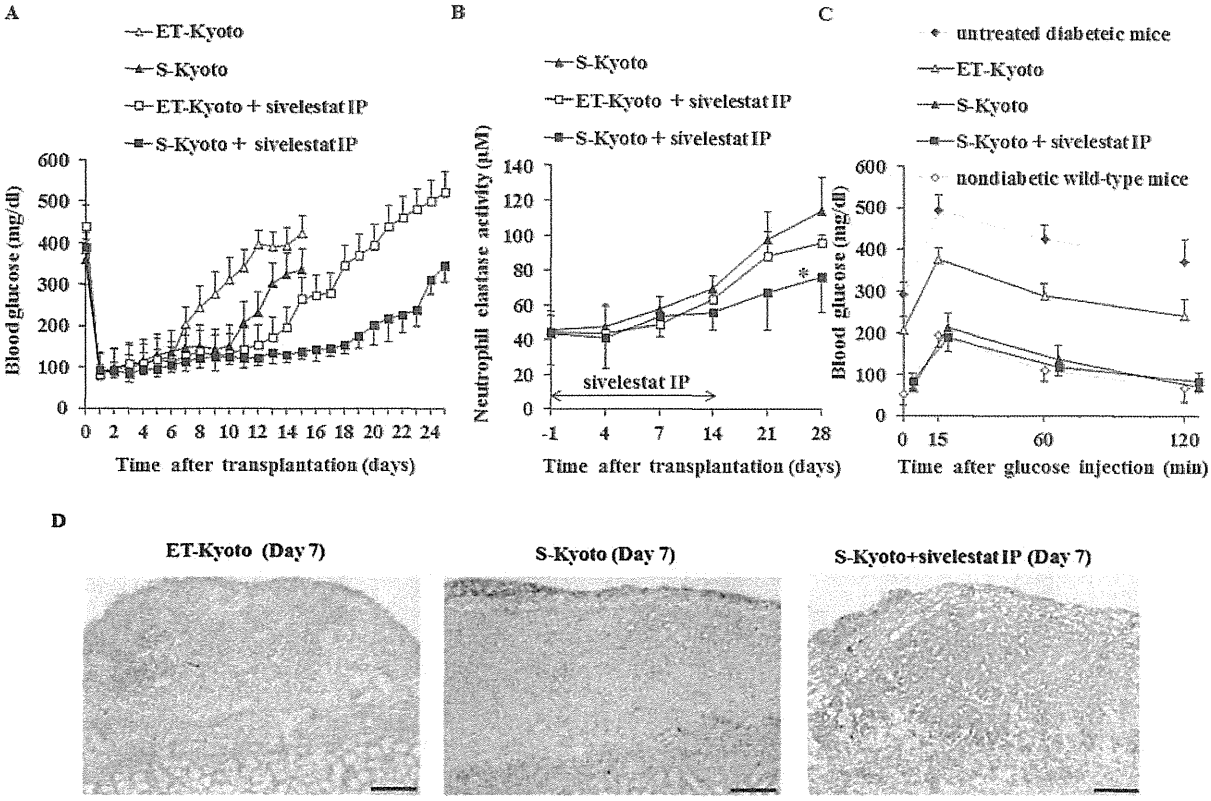

Figure 7. Results of in vivo transplant experiments. Islets were isolated using one of the isolation solutions (ET-Kyoto, S-Kyoto), then immediately transplanted (500 allogeneic islets) under the kidney capsule of diabetic mice. Sivelestat was injected intraperitoneally at 2 mg/day at 1 day before transplantation and every day until posttransplantation day 14. (A) Blood glucose levels of recipient mice transplanted with the islets. Data are mean ± SD of five independent mice. (B) Serum neutrophil elastase activity of recipient mice was measured at day 1 before transplantation and days 4, 7, 14, 21, 28 posttransplantation. Data are mean ± SD of three independent samples; $*p<0.05$, versus S-Kyoto. (C) IPGTT of recipient mice was performed at posttransplantation day 7. Blood glucose was measured in each group (nondiabetic wild-type mice, untreated diabetic mice, recipient mice transplanted with islets isolated by the use of ET-Kyoto, S-Kyoto, and S-Kyoto with sivelestat) before injection and at 15, 60, 120 min after injection. Data are mean ± SD of three independent mice. (D) Immunohistochemical analysis of insulin in a representative mouse kidney engrafted with islets was performed at posttransplantation day 7. Scale bars: 100 μm.

Table 3. Survival of Islet Allografts in Mice With Streptozotocin-Induced Diabetes

	Without Intraperitoneal Injection of Sivelestat		With Intraperitoneal Injection of Sivelestat	
	ET-Kyoto	S-Kyoto	ET-Kyoto	S-Kyoto
Graft survival (days)	6, 7, 8, 9	10, 11, 12, 13	12, 13, 14, 17, 20	18, 19, 20, 22, 26
Mean survival (days)	7.4 ± 1.1	11.2 ± 1.1¶	15.2 ± 3.3§	21.0 ± 3.2†

Data are mean ± SD of five independent experiments. ¶$p<0.01$, §$p<0.001$, compared with the ET-Kyoto isolation solution without intraperitoneal injection of sivelestat. †$p<0.001$, compared with the S-Kyoto isolation solution without intraperitoneal injection of sivelestat.

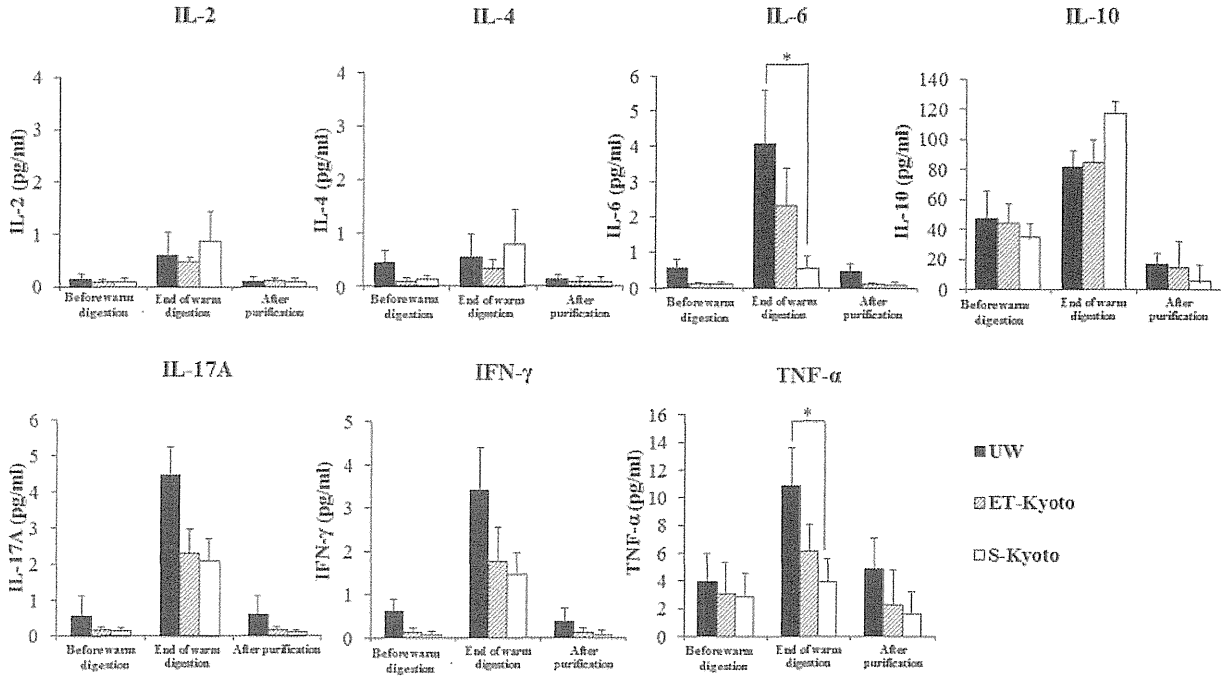

Figure 8. Assessment of proinflammatory cytokines in isolation solution during islet isolation. The levels of proinflammatory cytokines [interleukin (IL)-2, IL-4, IL-6, IL-10, IL-17A, interferon (IFN)-γ, tumor necrosis factor (TNF)-α] in the isolation solution were measured during islet isolation (before warm digestion, at the end of warm digestion, after purification). Data are mean±SD of four independent experiments; $^*p<0.05$.

significant increases were noted in the levels of other cytokines except IL-6 and TNF-α (Fig. 9). The serum levels of IL-6 and TNF-α were significantly lower in the sivelestat intraperitoneal (IP) group compared with nonsivelestat IP group at 7 and 14 posttransplantation days (Fig. 9).

DISCUSSION

Islet transplantation is currently one of the most attractive strategies for the treatment of type 1 diabetes. One important key to achieving successful insulin independence after islet transplantation is acquiring a sufficient donor islet mass (1,10). The number and quality of islets recovered from isolation are influenced by several factors (10). Tissue damage of donor pancreas starts to occur as early as the onset of brain death associated with hypotension, peripheral vasoconstriction, tissue ischemia, and release of stress hormones and inflammatory mediators (10,20,24,38). Moreover, at the time of procurement, donor pancreas is exposed to warm ischemia after donor cross-clamping and cold ischemia storage in preservation solution, such as UW, ET-Kyoto solution (23,40). Furthermore, during islet isolation, warm digestion, trauma, and hypoxia may cause cell damage in isolated islets similar to ischemia/reperfusion injury (IRI) of other transplant organs (10). Therefore, we need to design an efficient isolation method to reduce cell damage toward donor pancreata.

The major finding of the present study was identification of the crucial role of NE in islet isolation and transplantation. First, we showed a marked increase in NE activity during islet isolation, especially at the end of warm digestion by collagenase (Fig. 2C), and that NE was cytotoxic against isolated islets (Fig. 1A). Second, the addition of sivelestat to the isolation solution during islet isolation inhibited NE activity (Fig. 2C) and significantly improved islet yields, islet viability, and insulin function of isolated islets (Tables 1 and 2). Furthermore, we also showed that treatment of recipient animals with sivelestat significantly prolonged the survival of insulin-secreting islet allografts (Fig. 7A, Table 3).

In clinical liver transplantation, IRI, an exogenous antigen-independent inflammatory event, remains a major problem, because IRI causes early transplant graft failure and can lead to a higher incidence of both acute and chronic rejections (6,54,55). The mechanisms underlying liver IRI involve leukocyte accumulation and activation of neutrophils, Kupffer cells (macrophages), and T cells, secretion of proinflammatory cytokines and chemokines, complement activation, and activation of vascular cell adhesion molecules (49,51,53–55). Recent reports also indicated that the cross-talk interaction between NE and